Analysis of the Amount of Heat Flow Between Cooling Channels in Three Vented Brake Discs[1]

Análisis de la cantidad del flujo de calor entre canales de refrigeración en tres discos de frenos ventilados[2]

Ricardo Andrés García León[3]
Eduar Pérez Rojas[4]

[3] Industrial engineer, Universidad de Pamplona. Mechanical Engineer. Assistant professor, School of Engineering, Universidad Francisco de Paula Santander, Ocaña. Member of Research Group INGAP. E-mail: ragarcial@ufpso.edu.co

[4] Mechanical Engineer. Professor, School of Engineering, Universidad Francisco de Paula Santander, Ocaña. Member of Research Group INGAP. E-mail: eeperezr@ufpso.edu.co

Abstract

Introduction: the objective of this study was to analyze the behavior of the temperature, velocity and heat flow in the ventilation duct of three brake disc designs using computational fluid dynamics (CFD). **Methods**: the design software SolidWorks was used for the analysis. The three disc designs differed in geometry and application. The numerical results for the flow of heat through the ventilation channels were compared with mathematically obtained results. **Results**: the numerical results showed that the discs performed well under severe operating conditions (80 Km/h and an ambient temperature of 22°C). It is very important in brake disc design to select the appropriate geometry, particularly the number and the cross section of the ducts, and the type of material. **Conclusions**: numerical methods offer advantages for selecting the geometry and the material and for modeling the fluid flow to optimize the heat dissipation to provide the maximum performance for properly maintained components.

Resumen

Introducción: el objetivo de este estudio fue analizar el comportamiento de la temperatura, velocidad y flujo de calor en el conducto de ventilación de tres diseños de discos de freno utilizando la dinámica de fluidos computacional (CFD). **Métodos**: se utilizó el software de diseño Solid-Works para el análisis. Los tres diseños de disco diferían en geometría y aplicación. **Resultados**: los resultados numéricos para el flujo de calor a través de los canales de ventilación se compararon con los resultados obtenidos matemáticamente. Los resultados numéricos mostraron que los discos se desempeñaron bien bajo condiciones de operación severas (80 Km/h y una temperatura ambiente de 22°C). Es muy importante en el diseño del disco de freno seleccionar la geometría apropiada, particularmente el número y la sección transversal de los conductos, y el tipo de material. **Conclusiones**: los métodos numéricos ofrecen ventajas para seleccionar la geometría y el material y para modelar el flujo de fluido para optimizar la disipación de calor para proporcionar el máximo rendimiento para componentes adecuadamente mantenidos.

Keywords

Ventilation channels; CFD; heat flow; FEA; Disc brakes; friction; heat loss; temperature

Palabras Clave

Canales de ventilación; CFD; Flujo de Calor; FEA; Frenos de disco; Fricción; Pérdida de calor; Temperatura

1. Introduction

The braking system is undoubtedly the most important component in auto-mobiles for road safety because slowing and stopping of the vehicle and, conse-quently, the safety of the vehicle occupants depend on this system. Generally, 70% of the kinetic energy of the vehicle is absorbed by the front brakes, and the remainder is absorbed by the rear brakes. On most automobiles, the front wheels have disc brakes and the rear wheels have drum brakes. Friction is used to reduce the speed of the vehicle, where the friction is generated by hydraulic pressure that presses the brake pads against the cast iron discs. The brakes convert the vehicle kinetic energy to heat energy during braking, and the temperature of the brakes increases with the amount of friction. This heat dissipates rapidly to the surrounding air by convection (heat transfer between masses at different temperatures). The heat dissipation depends on the geometry of the disc and on the material. Environmental factors also affect the heat transfer. However, high heat accelerates corrosion. At high temperatures, radiation heat transfer occurs, which also dissipates the heat stored in the disk [1] [2]. Under these con-ditions, the functionality and the safety of the brakes can be compromised. It is important to note that disc brakes are less costly than drum brakes to maintain.

The geometry of the disks is chosen based on the load capacity and the op-eration of the vehicle, which is an important factor in the initial design phase. The discs should be designed to avoid overheating due to friction, taking into account the physical, mechanical and chemical properties. In certain cases, the materials selected may have properties that have negative effects on the brak-ing efficiency [3]. In designing ventilated disc brakes, it is very important to analyze the behavior of the surrounding fluid (air). The characteristics and the flow of the fluid at the surface of the disc can be studied to evaluate the effectiveness of the brakes and the heat dissipation by the disc surface and the ventilation channels [4]. The heat dissipation and the performance of ventilated disc brakes depend largely on the air flow over the surface and through the

ventilation channels of the discs, which can be studied using computational fluid dynamics (CFD). The design software SolidWorks offers modules for CFD analysis [5] [6].

Ventilated disc brakes are currently favored because of their heat dissipation characteristics. Recent research has shown that ventilated disks have high heat transfer rates because of turbulence, which results in higher temperatures and thus a larger heat transfer coefficient. Ventilated discs also have greater resistance to thermal deformation because of the uniform distribution of material, which reduces the thermal stresses within the disc. The stresses depend on the geometry of the disc and the ventilation channels [7] [8].

For heat transfer in brakes, steady flow of an incompressible fluid such as air is assumed. The temperature, the Nusselt number and suction and injection at the outlets and inlets affect the heat transfer. Recirculation of the surrounding fluid in the ventilation channels, which is essential for the dissipation of heat by the fluid, may or may not occur [9].

Heat-transfer analysis has shown that there are temperature gradients in the walls of the ventilation channels and thermal stresses in the walls that can lead to deformations that affect the flow in the channels. It is important to take into account these thermal distortions and their effects on performance in the design of a brake disc. CFD can assist in understanding the flow and the mode of heat transfer and thus assist in the process of designing components and geometries for the braking system [10] [11].

Heat in the brake discs of vehicles is transferred by natural convection, whereby a solid object subjected to a fluid flow parallel to its surface is cooled. Objects modeled with CAD software can be readily analyzed with CFD [12].

In research on ventilated disc brakes, the main objective in most cases has been to examine the heat flux to improve the heat dissipation to the surrounding environment. CFD analysis has been used to obtain predictions of the flow and the heat transfer, which were compared with experimental data available in the literature [13] [14]. Pre-processing is often accomplished using design software such as ANSYS or SolidWorks [15]. CFD has become increasingly important in the design of automotive components because of advances in hardware and software and numerical techniques to solve the equations of fluid flow. The interest of the automotive industry in CFD stems from the opportunity to improve vehicle performance, reduce the product cost and increase the product lifetime [16] [17] [18]. For the aforementioned reasons, the cooling of brake discs is an important area of research.

2. Materials and methods

Brake discs from three types of vehicles were selected. The vehicles were chosen based on the load capacity and the intended usage. The three vehicles were a Renault automobile, a Toyota pickup truck and a small bus manufactured by Mitsubishi (View Figures 1, 2 and 3) [19] [20].

The kinetic and potential energy of the vehicle are rapidly transformed into heat energy by the brakes. For the braking system to function properly, the heat generated must be dissipated as rapidly as possible so that successive braking does not overheat the system and thus compromise performance and safety. The movement of the vehicle allows dissipation of the heat by convection and radiation [21]. Heavy braking causes the temperature to rise to a certain limit, known as the saturation temperature, which depends on the thermal dissipation capacity of the brake disc. The saturation limit was not included in the analysis in the present study.

The physical and thermal properties of the discs were obtained. The disc materials were analyzed, and it was found that the discs consisted of nodular gray cast iron with laminar graphite, silicon and manganese. The physical and thermal properties of this material were determined by Cengel [22]:

Termal conductivity k = 41 J/s · m · ºC
Specific heat Cp = 434 J/kg · ºC
Density ρ = 8131 kg/m3
Thermal diffusivity α = 11.60 · 10⁶ m²/s
Heat transfer coefficient U = 32 J/s · m² · ºC

The change in temperature of a brake assembly can be approximated by the following expression:

$$\Delta T = \frac{E_{Total\ in\ Disc}}{m * C_p}$$

(1)

Where:
ΔT = Difference in temperature between the disc and the environment (ºC)
$E_{Total\ in\ Disc}$ = Kinetic energy absorbed by the disc (J)
M = Brake disc mass (kg)
C_p = Specific heat of the material

Equation 1 is a simplified model. In practice, however, additional variables are involved, and for that reason, it is unlikely that this model will produce values similar to experimental results. The values obtained from Eq. 1 for the three types of brake discs are shown in Table 1, where the energy was calculated assuming that the vehicle masses were 1250, 1950 and 2250 kg and the initial vehicle speed was 80 km/h.

Table 1. Change in disc temperature.

DISC	D1	D2	D3
ΔT (°C)	62	87	70

Source: authors' own elaboration

The temperature of the disk surface following braking T_1, was calculated using the following equation:

$$T_1 - T_\infty = \Delta T \tag{2}$$

Where T_∞ is the ambient temperature, 22°C. From Eqs. 1 and 2, the temperature of the surface of the brake disc can be calculated; the results are shown in Table 2.
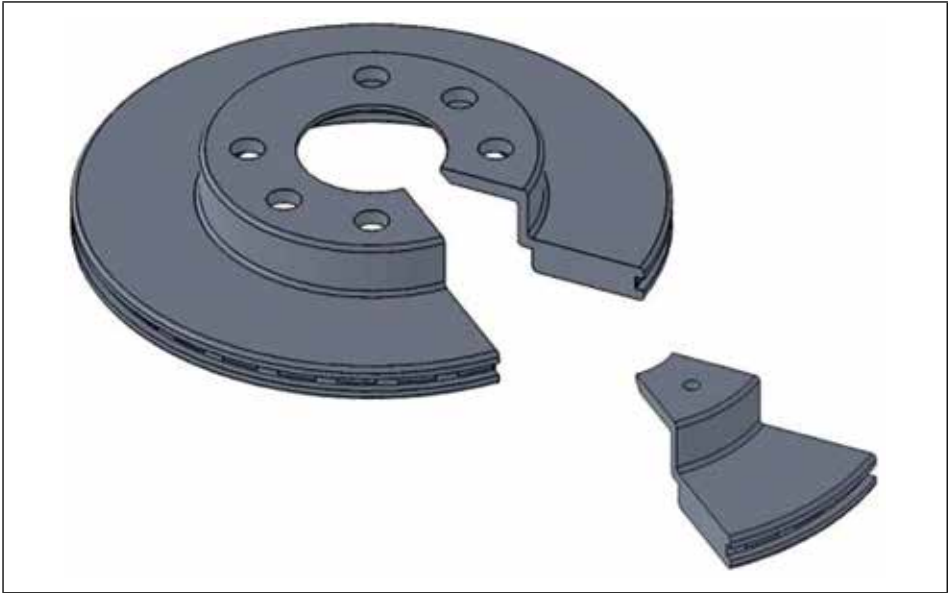
Table 2. Disc surface temperature.

| DISC	D1	D2	D3
T_1 (°C)	82	107	90

Source: authors' own elaboration

These results indicate that for a vehicle with a mass of 1250, 1950 or 2250 kg and a speed of 80 km/h in an environment of 22°C, the temperature reached by the brake discs in bringing the vehicle to a stop was 82, 107 or 90°C, respectively.

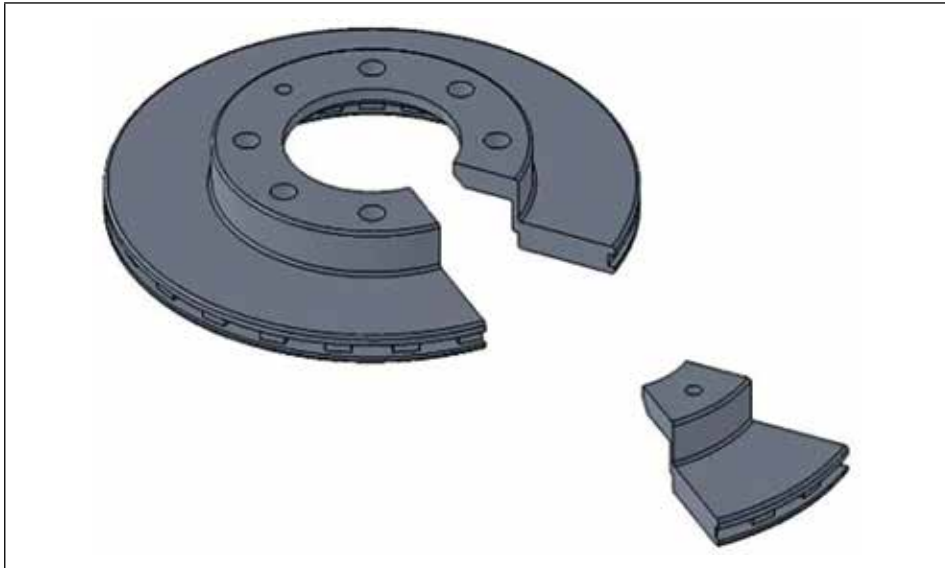Figure 1. Geometry of disc 1.

Source: authors' own elaboration

Figure 2. Geometry of disc 2
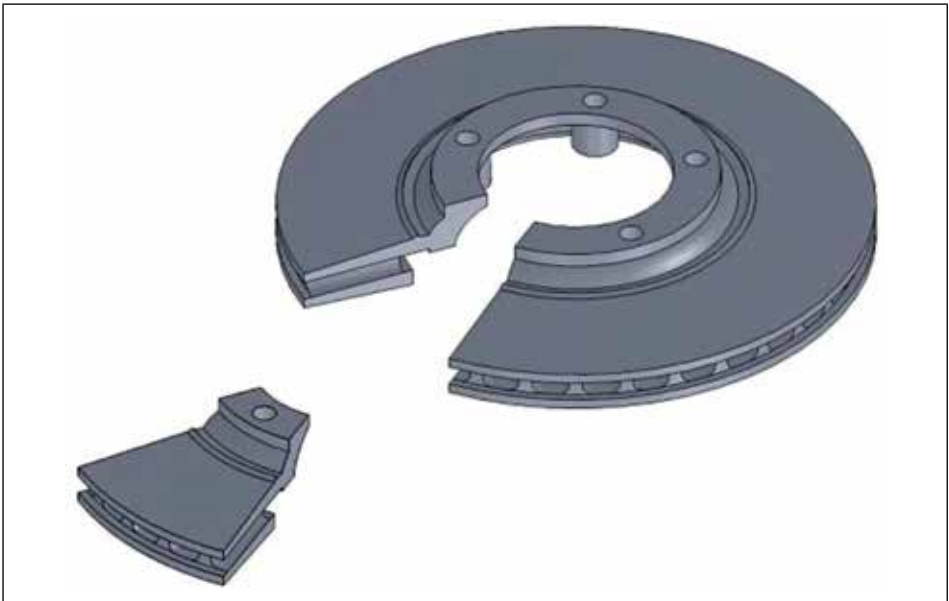
Source: authors' own elaboration

Figure 3. Geometry of disc 3

Source: authors' own elaboration

It is necessary to determine the air velocity at the inlets and outlets of the ducts in the brake discs. In each disc, the ducts all have identical geometries.

To calculate the velocities, the following relation from [12] for the air flow rate inside a duct was used:

$$Q = \pi * b_1 * D_1 * C_{1m} \tag{3}$$

Where:
Q = Fluid flow rate inside the duct (m³/s)
b_1 = Width of the impeller at the inlet (m)
D_1 = Inlet diameter (m)
C_{1m} = Absolute velocity of te fluid at te inlet of the duct (m/s)

By calculating the inlet and outlet velocities on the blades, the convection coefficient of the channels can be determined, as shown in [19].

In Figuress. 4, 5 and 6, the average dimensions of the ventilation ducts for the three types of discs used in the present study are shown.
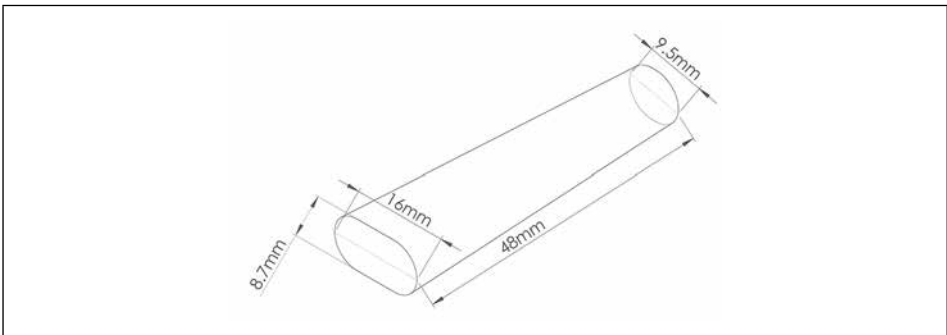
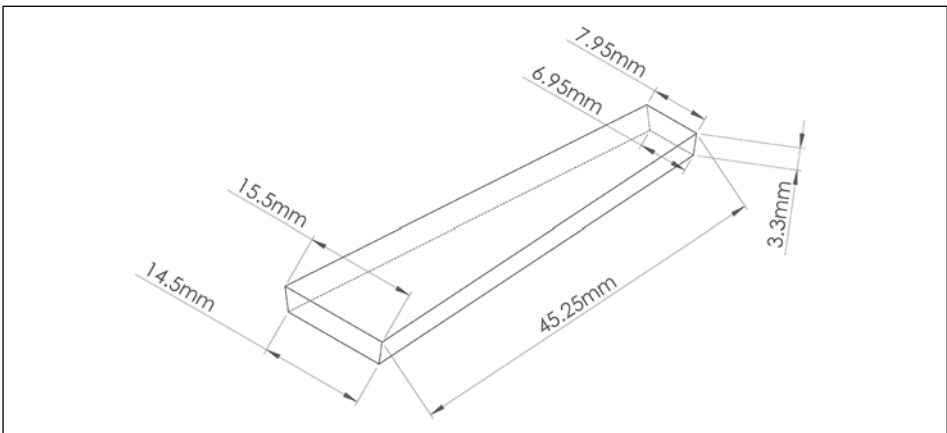Figure 4. Dimensions of the ventilation duct of brake disc 1
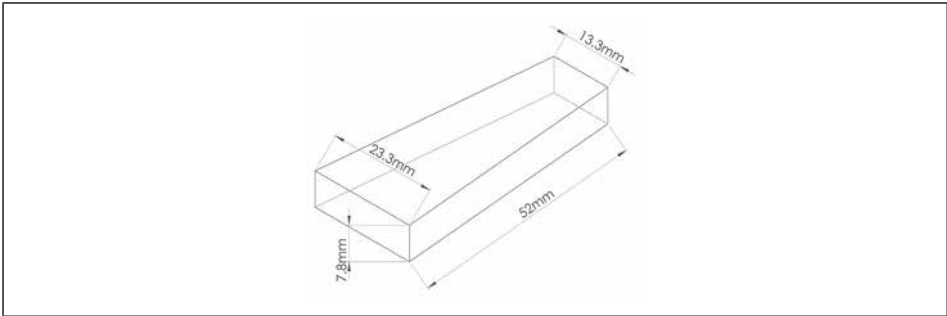
Source: authors' own elaboration

Figure 5. Dimensions of the ventilation duct of brake disc 2

Source: Authors' own elaboration

Figure 6. Dimensions of the ventilation duct of brake disc 3

Source: authors' own elaboration

Because the flow is radial, the absolute velocity of the fluid is equal to the lower component of the absolute velocity at the inlet; i.e.:

$$C_1 = C_{1m}$$

$$\alpha = 90°$$

Then, the absolute velocity in the duct is:

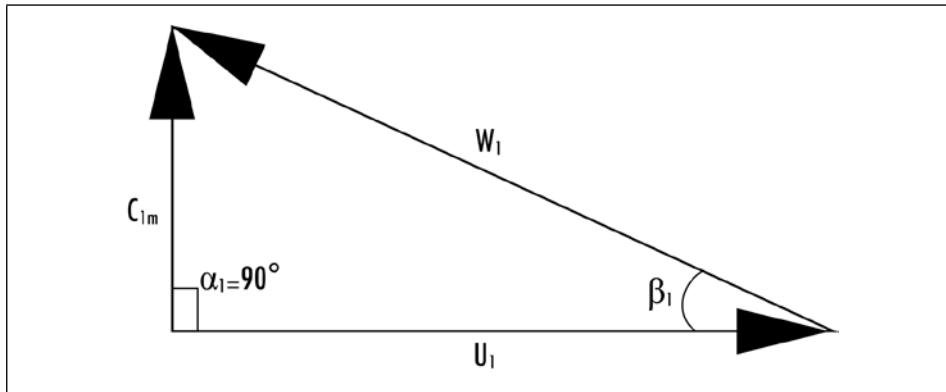$$u_1 = \frac{\pi * D_1 * n}{60}$$

(4)

u_1 = Absolute velocity at the inlet of the duct (m/s)
D_1 = Inlet Diameter (m)
N = Rotation speed (RPM)

Figure 7. Velocity vector of air at the inlet.

Source: authors' own elaboration

The units presented in the previous Figures. 4, 5 and 6 were converted to meters for the purposes of mathematical calculations, the results of which are shown in Table 3.

Table 3. Dimensions and velocities at the duct inlet.

DISC	D1	D2	D3
Inlet diameter D_1 (m)	0.1352	0.1226	0.1801
Width of the impeller at the inlet D_1 (m)	0.00745	0.0095	0.0133
Absolute velocity u_1 (m/s)	5.0460	4.2397	5.2441

Source: authors' own elaboration

To calculate the angle β_1 of the velocity vector, the following relation was used [19]:

$$\text{Tan}\,\beta_1 = \frac{C_1}{u_1} \tag{5}$$

The relative velocity of the fluid with respect to the duct is given by

$$w_1 = \sqrt{C_1^2 + u_1^2} \tag{6}$$

The flow rates were then calculated using Eq. 3, and the results are shown in Table 4.

Table 4. Fluid flow rates through the ducts.

DISC	D1	D2	D3
Q (m³/s)	0.01596	0.01551	0.03946

Source: authors' own elaboration

According to the continuity equation, the flow rate through the duct is constant; only the velocity varies. The width of the impeller at the outlet is $b_2 = 0.015$ m for disc D1 and the outer diameter is $D_2 = 0.2632$ m for disc D1, and therefore, the flow rate can be expressed as:

$$Q = \pi * b_2 \,{}^*D_2 \,{}^*C_{2m} \tag{7}$$

Where:
Q = Fluid flow rate inside the duct (m³/s)
b_2 = Width of the impeller at the outlet (m)

D_2 = Outlet diameter (m)
C_{2m} = Absolute velocity of the fluid at the outlet (m/s)

Figure 8. Velocity vector of air at the outlet.
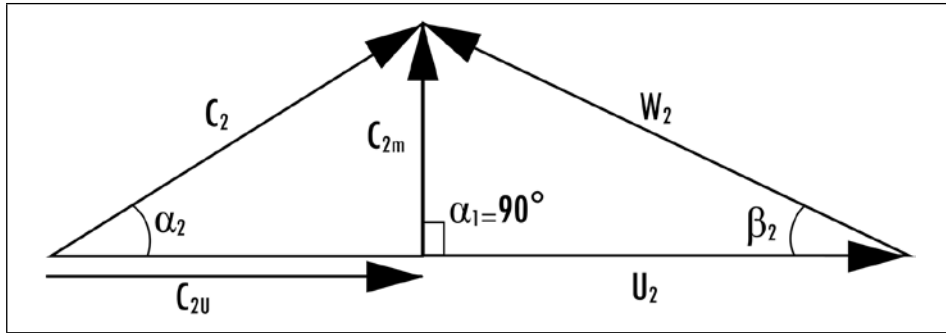
The absolute velocity of the fluid at the outlet was calculated with the following equation (View Figure 8):

$$u_2 = \frac{\pi * D_2 * n}{60}$$

(8)

Where:
u_2 = Absolute velocity at the outlet of the blade (m/s)
D_2 = Outlet diameter (m)
N = Rotation speed (RPM)

To calculate the angle β_2 of the velocity vector, the following relation was used:

$$\text{Tan}\,\beta_2 = \frac{C_{2m}}{u_2}$$

(9)

The relative velocity of the fluid with respect to the duct can be obtained using the following equation:

$$w_2 = \sqrt{C_{2m}^2 + u_2^2}$$

(10)

The peripheral component of the absolute velocity at the outlet of the duct can be obtained with the following equation:

$$C_{2u} = u_2 \frac{C_{2m}}{\operatorname{Tan}\beta_2}$$

$$(11)$$

The absolute velocity of the fluid at the outlet can be obtained with the following equation:

$$C_2 = \sqrt{C_{2u}^2 + C_{2m}^2}$$

$$(12)$$

To calculate the angle α_2 of the velocity vector, the following relation was used:

$$\operatorname{Tan}\alpha_2 = \frac{C_{2m}}{C_{2u}}$$

$$(13)$$

With the duct inlet and outlet velocities, the heat transfer by convection can be calculated.

The mean velocity of the fluid was calculated from the following equation:

$$V_m = \frac{C_{1m} + C_{2m}}{2}$$

$$(14)$$

Table 5 shows the velocities calculated from Eq. 14.

Table 5. Mean velocity of the fluid

DISC	D1	D2	D3
V_m (m/s)	3.24	2.72	3.52

Source: authors' own elaboration

The average hydraulic diameter is:

$$D_h = \frac{D_{h_I} + D_{h_o}}{2}$$

$$(15)$$

Where:

D_h = Hydraulic diameter (m)

D_{h_i} = Inlet hydraulic diameter (m)

D_{h_o} = Outlet hydraulic diameter (m)

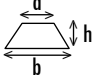The inlet hydraulic diameter for a rectangular duct can be expressed as:
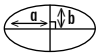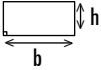
$$D_h = \frac{4 * A_C}{p}$$

(16)

Where:

A_C = Cross- sectional area (m²)

p = Perimeter of the cross section (m²)

Table 6. Geometries, cross-sectional areas, and hydraulic diameters of the ducts

DISC	D1	D2	D3
Cross section	Trapezoid	Ellipse	Rectangle
Channel geometry			
Area (m²)	$\dfrac{(b+a)*h}{2}$	$\pi * a * b$	$a * h$
Perimeter (m²)	$b + a + 2h$	$2\pi\sqrt{\dfrac{a^2 + b^2}{2}}$	$2(a + h)$
Inlet dimensions (m)	a = 0.00695 b = 0.00795 h = 0.00344	a = 0.00475 b = 0.00425	a = 0.0133 h = 0.0078
Outlet dimensions (m)	a = 0.01450 b = 0.01550 h = 0.00344	a = 0.00800 b = 0.00425	a = 0.0233 h = 0.0078
D_{h_I} (m)	0.004500	0.008958	0.009833
D_{h_o} (m)	0.005600	0.010600	0.011680
D_h (m)	0.005050	0.009779	0.010750

Source: authors' own elaboration

The Reynolds number is given by the following equation:

$$Re = \frac{V_m * D_h}{\upsilon}$$

(17)

Where:
Re = Reynolds number (nondimensional)
V_m = Mean fluid velocity (m/s)
D_h = Hydraulic diameter (m)
υ = Kinematic viscosity of the air (m²/s)

For a temperature of 51 °C, the Reynolds number is less than 10,000, and therefore, the flow is laminar. The Nusselt number was obtained from [22] using the dimensions of the duct at the inlet. The Nusselt number was interpolated with the ratio a/b assuming a constant temperature; the results are shown in Table 7.

Table 7. Nusselt number for convection between the ducts.

DISC	D1	D2	D3
Nu	3.817	3.6672	3.2690

Source: authors' own elaboration

The convection coefficient, shown in Table 8, is given by the following equation [22]:

$$h = \frac{k}{d_h} * Nu$$

(18)

Table 8. Convection coefficient for the flow in the ducts.

DISC	D1	D2	D3
h (W/m²* °C)	21.22	10.62	8.42

Source: authors' own elaboration

The surface area in the duct is given by:

$$A_s = P * d$$

(19)

Where:

A_S = Surface area in the duct (m²)

d = Length of the duct (m)

p = Perimeter of the cross section (m²)

Then, we can obtain Table 9.

Table 9. Lengths and surface areas of the ducts.

DISC	D1	D2	D3
d (m)	0.04525	0.04800	0.05200
A_{S_i} (m²)	0.0009862	0.001358	0.002194
A_{S_o} (m²)	0.0016690	0.001929	0.003234
A_S (m²)	0.0013270	0.001643	0.002714

Source: authors' own elaboration

The heat loss rate, shown in Table 10, can be calculated with the following equations:

$$\dot{Q}_{Duct} = h * A_S * \Delta T \tag{21}$$

$$\dot{Q}_{Duct} = h * A_S * \left(T_s - T_\infty \right) \tag{22}$$

Table 10. Duct heat loss rates.

DISC	D1	D2	D3
$\dot{Q}_{Ducto}$ (W)	1.7459	1.5186	1.6008

Source: authors' own elaboration

The total heat losses in the ventilation ducts of the discs were calculated and are shown in Table 11.

Table 11. Total heat loss in the ventilation ducts.

DISC	D1	D2	D3
Number of ducts	30	36	24
$\dot{Q}_{Total\ Ducts}$ (W)	52.37	54.66	38.41

Source: authors' own elaboration

3. Results of the numerical analysis

A numerical analysis was conducted to estimate the heat loss. A ventilated disc dissipates heat faster than a solid disc or a drum because of the differences in the geometry. The analysis was conducted using SolidWorks with the CFD library.

The initial conditions for the numerical analysis are shown in Table 12.

Table 12. Boundary conditions for the numerical analysis.

DISC	D1	D2	D3
Fluid velocity	3.24	2.72	3.52
Fluid temperature (°C)	22	22	22
Disc temperature (°C)	82	107	90
Material roughness (gray cast iron)	0.1 μm	0.1 μm	0.1 μm
Simulation time	60 s	60 s	60 s

Source: authors' own elaboration

The disc brake material was gray cast iron, which was determined by a chemical analysis. The roughness and the initial temperature were required for the analysis.

A mesh was constructed using irregularly distributed nodes, as shown in Figure 9.

Figure 9. Type of mesh used for the discs.
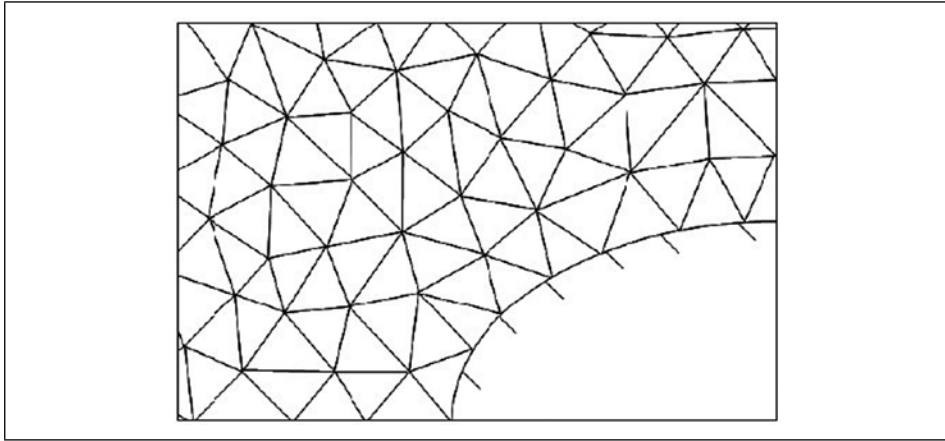
Source: authors' own elaboration

To model the fluid flow, SolidWorks solves the Navier-Stokes equations, which are formulations of the laws of conservation of mass, momentum and energy. These equations are given in Eqs. $20 - 32$ [23] [24]:

To calculate the behavior of high-velocity compressible flows and shock waves, the following energy equation is used:

$$\frac{\partial \rho}{\partial t} + \frac{\partial \left(\rho u_i \right)}{\partial x_i} = 0 \tag{20}$$

$$\frac{\partial \left(\rho u_i \right)}{\partial t} + \frac{\partial}{\partial x_i} \left(\rho u_i u_j \right) + \frac{\partial P}{\partial x_i} = \frac{\partial}{\partial x_j} \left(\tau_{ij} + \tau_{ij}^R \right) + S_i \tag{21}$$

$$\frac{\partial \rho H}{\partial t} + \frac{\partial \rho u_i H}{\partial x_i} = \frac{\partial}{\partial x_j} \left(u_i \left(\tau_{ij} + \tau_{ij}^R \right) + q \right) + \frac{\partial \rho}{\partial t} - \tau_{ij}^R \frac{\partial u_i}{\tau x_i} + \rho \varepsilon + S_i u_i + Q_H$$

$$H = h + \frac{u^2}{2} \tag{22}$$

$$\frac{\partial \rho E}{\partial t} + \frac{\partial \rho u_i \left(E + \frac{p}{\rho} \right)}{\partial x_i} = \frac{\partial}{\partial x_j} \left(u_i \left(\tau_{ij} + \tau_{ij}^R \right) + q_i \right) + \frac{\partial \rho}{\partial t} - \tau_{ij}^R \frac{\partial u_i}{\partial x_i} + \rho \varepsilon + S_i u_i + Q_H$$

$$E = e + \frac{u^2}{2}$$
(23)

$$\frac{\partial \rho k}{\partial t} + \frac{\partial \rho k u_i}{\partial x_i} = \frac{\partial}{\partial x_j}\left(\left(\mu + \frac{\mu_i}{\sigma_k}\right)\frac{\partial k}{\partial x_i}\right) + \tau_{ij}^R \frac{\partial u_i}{\partial x_j} - \rho\varepsilon + \mu_i P_B$$
(24)

$$\frac{\partial \rho k}{\partial t} + \frac{\partial \rho k u_i}{\partial x_i} = \frac{\partial}{\partial x_j}\left(\left(\mu + \frac{\mu_i}{\sigma_k}\right)\frac{\partial\varepsilon}{\partial x_i}\right) + C_{\varepsilon 1}\frac{\varepsilon}{k}\left(f_1\tau_{ij}^R\frac{\partial u_i}{\partial x_j} + C_{\varepsilon 1}\mu_i P_B\right) - f_1 C_{\varepsilon 2}\frac{\rho\varepsilon^2}{k}$$
(25)

$$\tau_{ij} = \mu S_{ij}, \qquad \tau_{ij}^R = \mu S_{ij} - \frac{2}{3}\rho k\delta_{ij}, \qquad S_{ij} = \frac{\partial u_i}{\partial x_j} + \frac{\partial u_j}{\partial x_i} - \frac{2}{3}\delta_{ij}\frac{\partial k}{\partial x_k}$$
(26)

$$P_B = -\frac{g_i}{\sigma_B}\frac{1}{\rho}\frac{\partial \rho}{\partial x_1}$$
(27)

Where:
$C_u = 0{,}09$
$C_{\varepsilon 1} = 1.44$
$C_{\varepsilon 2} = 1$
$\sigma_k = 0.9$
$\sigma_\varepsilon = 1$
$C_B = 1$ if $P_B > 0$
$C_B = 1$ if $P_B < 0$

The turbulent viscosity is determined from:

$$\mu_1 = f_\mu \frac{C_\mu \rho k^2}{\varepsilon}.$$
(28)

The Lam-Bremhorst damping function f_μ is determined from:

$$f_\mu = \left(1 - e^{-0.025 R_y}\right)^2\left(1 + \frac{20.5}{R_t}\right)$$
(29)

Where:

$$R_y = \frac{\rho \sqrt{Ky}}{\mu} \tag{30}$$

$$R_t = \frac{\rho k^2}{\mu \varepsilon} \tag{31}$$

And y is the distance from the point to the wall.

The Lam-Bremhorst damping functions f_1 and f_2 are determined from the following equation:

$$f_1 = 1 + \left(\frac{0.05}{f\mu}\right)^3, f_2 = 1 - e^{R_t^2} \tag{32}$$

The Lam-Bremhorst damping functions f_μ, f_1 and f_2 reduce the turbulent viscosity and the turbulent energy. These functions also increase the turbulence dissipation capacity when the Reynolds number is based on the average speed of the fluctuations and the distance from the wall is very small.

For $f_u = f_1 = f_2 = 1$, the equations reduce to the k-ε model.

The heat flow is defined by:

$$q_i = \left(\frac{\mu}{Pr} + \frac{\mu_i}{\sigma_c}\right)\frac{\partial h}{\partial x_i}, \qquad i = 1,2,3 \tag{33}$$

Where $\sigma_c = 0.9$, Pr is the Prandtl number and h is the thermal enthalpy. The numerical model was defined by specifying the geometry and the initial conditions. All of the data for these conditions were defined directly in the software.

SolidWorks was used to calculate two quantities in the discs, the heat conduction and the electric current, with the resulting Joule effect as the heat source in the energy equation.

The heat transfer in the solid and the fluid and the energy exchange between the two (conjugation of heat transfer) was simulated by the CFD software. Heat transfer in fluids is described by the energy equation (Eqs. 22 and 23), in

which the heat flux is defined by Eq. 33. Heat conduction in solids is described by the following equation:

$$\frac{\partial \rho e h}{\partial t} = \frac{\partial}{\partial x_1}\left(\lambda_i \frac{\partial T}{\partial x_i}\right) + Q_H \tag{34}$$

Where:
e = Specific internal energy, given by $e = c \cdot T$, where c is the specific heat
Q_h = Rate of specific heat emission per unit volume
λ_i = Values of the thermal conductivity tensor

It was assumed that the thermal conductivity tensor was diagonal in the coordinate system used in this study.

For an isotropic material, $\lambda_1 = \lambda_2 = \lambda_3 = \lambda$. In the presence of an electric current, Q_h includes the specific heat emission from the Joule effect Q_j. The heat from the Joule effect is defined as $Q_j = r \cdot j_2$, where r is the electrical resistivity and j is the electric current density. The vector for the electric current density is

$$i = -\left(\frac{1}{r_{11}}\frac{\partial \varphi}{\partial x_1}, \frac{1}{r_{22}}\frac{\partial \varphi}{\partial x_2}, \frac{1}{r_{33}}\frac{\partial \varphi}{\partial x_3}\right) \tag{35}$$

These terms can be determined from the electrical potential $\varphi[V]$ using the steady-state Laplace equation:

$$\frac{\partial}{\partial x_i}\left(\frac{1}{r_{ij}}\frac{\partial \varphi}{\partial x_i}\right) = 0 \tag{36}$$

As the disc cools, the disc temperature settles at the ambient temperature, which occurs between approximately 40 and 60 minutes for the discs subjected to the assumed loads and operating conditions. The numerical results can be compared with the analytical results in the literature for the given conditions.

The results obtained demonstrate the heat dissipation in a transient state for one instant of time, as can be seen in Figure 10.

Figure 10. Transient heat dissipation for one instant of time
(temperature map of the fluid for 60 s).

DISC	CFD ANALYSIS
D1	
D2	
D3	
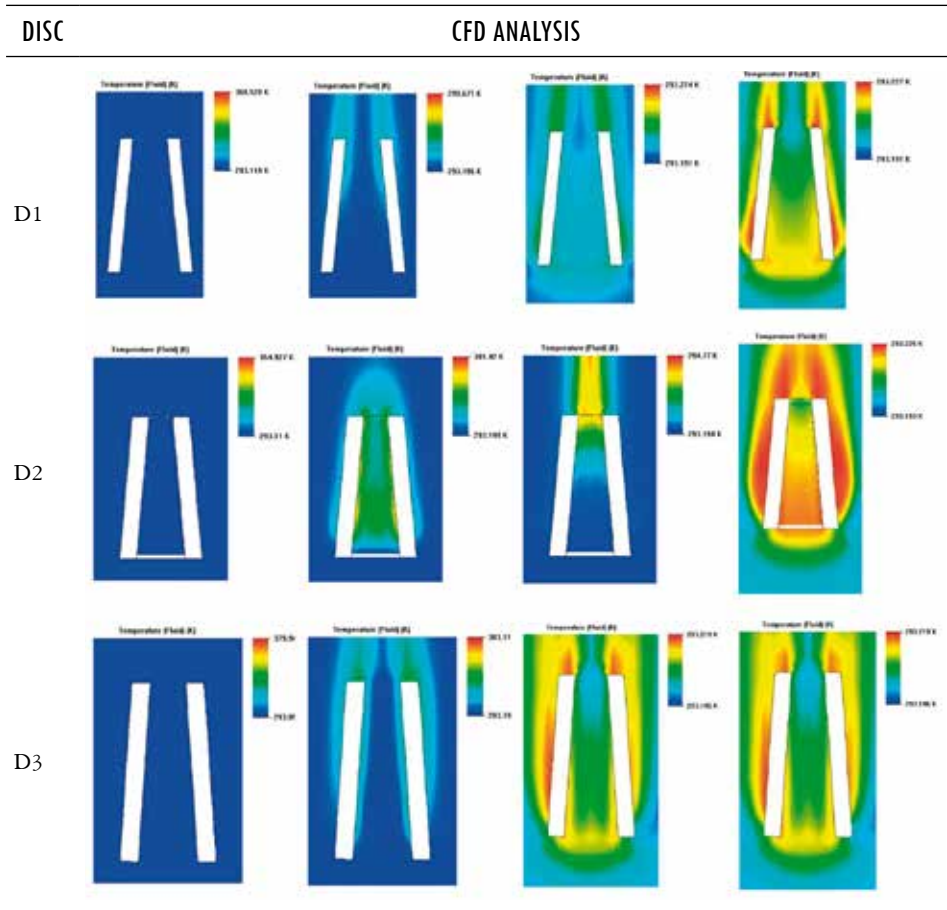
Source: authors' own elaboration

With time, the air dissipates heat more rapidly, which is indicated in red in each of the figures. It can be observed that disc D2 was the most effective in dissipating heat to the surrounding medium. Disc D2 had a greater number of channels (36) and satisfies the operational requirements for which it was designed, dissipating 54.66 W at a temperature of approximately 107 °C. Disc D1 satisfied the heat dissipation requirements, dissipating 52.32 W at a temperature of approximately 82 °C, but its difference lies in the number of channels (30), which makes the system geometry more efficient.

4. Conclusions

Most modern road vehicles have ventilated disc brakes in all four wheels because of their effectiveness, and thus, the heat transfer characteristics of brake discs are of interest. Drum brakes, which can be found on the rear axles of some vehicles, are subject to problems such as a lack of heat dissipation, moisture and the corrosion that results from inefficient braking because the friction surfaces are enclosed and heat dissipation is inhibited.

A numerical analysis was performed using SolidWorks with the CFD library for the three brake disc designs to study the temperature of the air inside the ventilation channels. Among the three designs, the Toyota pickup truck disc, which had an elliptical duct cross section, was found to have the best heat transfer characteristics for the assumed loads and operating conditions.

The dissipation of heat in disc brakes obviously depends on the disc geometry, as can be observed in the results of the analysis, in addition to the operating conditions.

References

[1]   R. A. García León, M. A. Acosta Pérez, and E. Flórez Solano, "Análisis del comportamiento de los frenos de disc de los vehículos a partir de la aceleración del proceso de corrosión," *Tecnura*, vol. 19, no. 45, pp. 53–63, 2015.

[2]   S. Hirasawa, T. Kawanami, and K. Shirai, "Numerical analysis of convection heat transfer on high-temperature rotating disk at bottom surface of air flow duct," in *ASME International Mechanical Engineering Congress and Exposition, Proceedings (IMECE)*, 2014, vol. 8A.

[3]   L. S. Bocîi, "The influence of braking time on heat flow through the friction surfaces of the friction elements of disk brakes for railway vehicles," *Transport*, vol. 26, no. 1, pp. 75–78, 2011.

[4]   H. B. Yan, S. S. Feng, X. H. Yang, and T. J. Lu, "Role of cross-drilled holes in enhanced cooling of ventilated brake discs," *Appl. Therm. Eng.*, vol. 91, pp. 318–333, 2015.

[5]   Z. Chi, Y. He, and G. Naterer, "Convective heat transfer optimization of automotive brake discs," *SAE Int. J. Passeng. Cars - Mech. Syst.*, vol. 2, no. 1, pp. 961–969, 2009.

[6]   F. Klimenda, J. Soukup, and J. Kampo, "Heat distribution in disc brake," in *AIP Conference Proceedings*, 2016, vol. 1745.

[7]   E. Palmer, R. Mishra, and J. Fieldhouse, "An optimization study of a multiple-row pin-vented brake disc to promote brake cooling using computational fluid dynamics," *Proc. Inst. Mech. Eng. Part D J. Automob. Eng.*, vol. 223, no. 7, pp. 865–875, 2009.

[8]   A. Nagarajan and M. R. Narayanan, "Maximization of efficiency for disk brake material using composite material by modelling and analysis," *Int. J. Control Theory Appl.*, vol. 9, no. 6, pp. 2793–2798, 2016.

[9]   H. G. Sharma and K. R. Singh, "Heat transfer in the flow of a second-order fluid between two enclosed rotating discs with uniform suction and injection.," *Indian J. Technol.*, vol. 23, no. 7, pp. 247–255, 1985.

[10] Y.-H. Ho, M. M. Athavale, J. M. Forry, R. C. Hendricks, and B. M. Steinetz, "Numerical simulation of secondary flow in gas turbine disc cavities, including conjugate heat transfer," in *ASME 1996 International Gas Turbine and Aeroengine Congress and Exhibition, GT 1996*, 1996, vol. 1.

[11] W. Wu, Z. Xiong, J. Hu, and S. Yuan, "Application of CFD to model oil-air flow in a grooved two-disc system," *Int. J. Heat Mass Transf.*, vol. 91, pp. 293–301, 2015.

[12] B. Watel, S. Harmand, and B. Desmet, "Influence of convective heat exchange on a rotating disc in superimposed air flow - comparison between heat pipe and solid discs," *J. Enhanc. Heat Transf.*, vol. 7, no. 4, pp. 259–272, 2000.

[13] S. Manohar Reddy, J. M. Mallikarjuna, and V. Ganesan, "Flow and heat transfer analysis through a brake disc - A CFD approach," in *American Society of Mechanical Engineers, Heat Transfer Division, (Publication) HTD*, 2006.

[14] S. M. Reddy, J. M. Mallikarjuna, and V. Ganesan, "Flow and heat transfer analysis of a ventilated disc brake rotor using CFD," *SAE Tech. Pap.*, 2008.

[15] T. K. R. Rajagopal, R. Ramachandran, M. James, and S. C. Gatlewar, "Numerical investigation of fluid flow and heat transfer characteristics on the aerodynamics of ventilated disc brake rotor using CFD," *Therm. Sci.*, vol. 18, no. 2, pp. 667–675, 2014.

[16] M. N. Dhaubhadel, "CFD applications in the automotive industry (invited keynote presentation)," *Am. Soc. Mech. Eng. Fluids Eng. Div. FED*, vol. 239, pp. 473–480, 1996.

[17] J. Wurm, M. Fitl, M. Gumpesberger, E. Väisänen, and C. Hochenauer, "Novel CFD approach for the thermal analysis of a continuous variable transmission (CVT)," *Appl. Therm. Eng.*, vol. 103, pp. 159–168, 2016.

[18] M. Pevec, I. Potrc, G. Bombek, and D. Vranesevic, "Prediction of the cooling factors of a vehicle brake disc and its influence on the results of a thermal numerical simulation," *Int. J. Automot. Technol.*, vol. 13, no. 5, pp. 725–733, 2012.

[19] C. Mataix, *Mecánica de Fluidos y Maquinas Hidraulicas. Segunda Edición*, Ediciones . Madrid, España, 1986.

[20] R. A. García León, "Evaluación del comportamiento de los frenos de disc de los vehículos a partir del análisis de la aceleración del proceso de corrosión.," Universidad Francisco de Paula Santander Ocaña, 2014.

[21] L. Pan, J. Han, Z. Li, Z. Yang, and W. Li, "Numerical simulation for train brake disc ventilation," *Beijing Jiaotong Daxue Xuebao/Journal Beijing Jiaotong Univ.*, vol. 39, no. 1, pp. 118–124, 2015.

[22] Y. Cengel, *Tansferencia de calor y masa. Un enfoque práctico. Tercera edición.* México: McGraw-Hil, 2007.

[23] A. Sobachkin, G. Dumnov, and A. Sobachkin, "Base numérica de CFD integrada en CAD. Informe Técnico.," *SolidWorks*, 2014.

[24] A. Thuresson, "CFD and Design Analysis of Brake Disc," Charlmers University Of Tecnology, 2014.